JOURNAL OF THEORETICAL
AND APPLIED MECHANICS
1, **39**, 2001

NUMERICAL SIMULATION OF THE AIRCRAFT FLIGHT AFTER ENCOUNTERING A MICROBURST WINDSHEAR

RAFAŁ DEPTUŁA
JERZY MARYNIAK

Insitute of Aeronautics and Applied Mechanics, Warsaw University of Technology
e-mail: rafald@meil.pw.edu.pl

A physical and mathematical modelling of the microburst effect on aircraft behaviour is presented in the paper. Dynamics equations of the aircraft motion are derived in a plane-fixed co-ordinate system using the Boltzmann-Hamel formalism for material systems with holonomic constraints. The aircraft is treated as a six-degree-of-freedom rigid body. For calculating of aerodynamic forces and moments the rules of quasi-stationary aerodynamics were employed. The windshear velocity field is described by the 3D mathematical Bray' model which was applied basing on the meteorological data resulting from the Joint Airport Weather Studies Project. The influence of local parameters of the microburst was introduced into the equations of flying object motion in terms of three instantaneous linear components of wind velocity and the three angular ones. Computations were made taking the PZL I-22 "Iryda" as a test aircraft.

Key words: flight dynamics, flight simulation

Notation

c	–	mean aerodynamic chord
g	–	gravitational acceleration
J_x, J_y, J_z	–	moments of inertia
J_{xy}, Jyz, J_{xz}	–	moments of inertia with respect to a plane
$J_{T()}$	–	moment of inertia of the engine-turbocompressor assembly
m	–	aircraft mass
S	–	lifting surface
S_x, S_y, S_z	–	static moments

t	–	time
$T_{()}$	–	thrust
$\boldsymbol{V}_A$	–	aircraft velocity relative to the atmosphere
W_x, W_y, W_z	–	wind speed vector components
$\boldsymbol{\Lambda}_V$	–	transformation matrix
α	–	angle of attack with the air motion considered
β	–	angle of sideslip with the air motion considered
$\boldsymbol{\Omega}_A$	–	relative angular velocity of the aircraft
$\boldsymbol{\Omega}_{wind}$	–	angular velocity of the air mass
$\varphi_{Ty()}, \varphi_{Tz()}$	–	angles, the axes of $Oxyz$ co-ordinate system make with the thrust axis.

The term "wind field" stands for the vector field of wind velocity, and the subscript g indicates that the quantity is measured in the inertial co-ordinate system.

1. Introduction

The paper presents mathematical and physical modelling of the influence a low-level windshear exerts on the dynamics of the PZL I-22 "Iryda" aircraft. This aircraft was chosen for simulation purposes since its aerodynamic characteristics are well known. The method used in the paper is a classic approach to dynamical analysis of a flying rigid body. Numerical simulation was performed for a horizontal steady off-center flight through the microburst. The results obtained are presented in the form of diagrams..

2. Mathematical model of a microburst

A mature stage of the microburst was idealised to resemble the wind-flow patterns given in meteorological microburst data resulting from the Joint Airport Weather Studies (JAWS) Program. The influence of the parameters, which characterise the microburst on the equations of aircraft motion, is introduced via consideration of:

- instantaneous linear components of wind velocity vector,
- instantaneous angular components of the wind field rotation vector.

The velocity of an aircraft relative to the atmosphere is represented by the relationship

$$\boldsymbol{V}_A = \boldsymbol{V}_0 - \boldsymbol{W}_{wind} \tag{2.1}$$

The relative angular velocity of an aircraft is given by

$$\boldsymbol{\Omega}_A = \boldsymbol{\Omega}_{airplane} - \boldsymbol{\Omega}_{wind} \tag{2.2}$$

The rotation vector $\boldsymbol{\Omega}_{wind}$ is the rotation of the wind field relative to the inertial frame of reference. Physically, this rotation can be viewed as a rotation of "rigid" air mass, which is brought about by fluid stresses. Thus, $\boldsymbol{\Omega}_{wind}$ can be written as follows

$$\boldsymbol{\Omega}_{wind} = \begin{bmatrix} P_W \\ Q_W \\ R_W \end{bmatrix} = \frac{1}{2}\mathrm{rot}\boldsymbol{W} = \frac{1}{2}\boldsymbol{\Lambda}_V \begin{bmatrix} \boldsymbol{i} & \boldsymbol{j} & \boldsymbol{k} \\ \dfrac{\partial}{\partial x} & \dfrac{\partial}{\partial y} & \dfrac{\partial}{\partial z} \\ W_x & W_y & W_z \end{bmatrix}_g \tag{2.3}$$

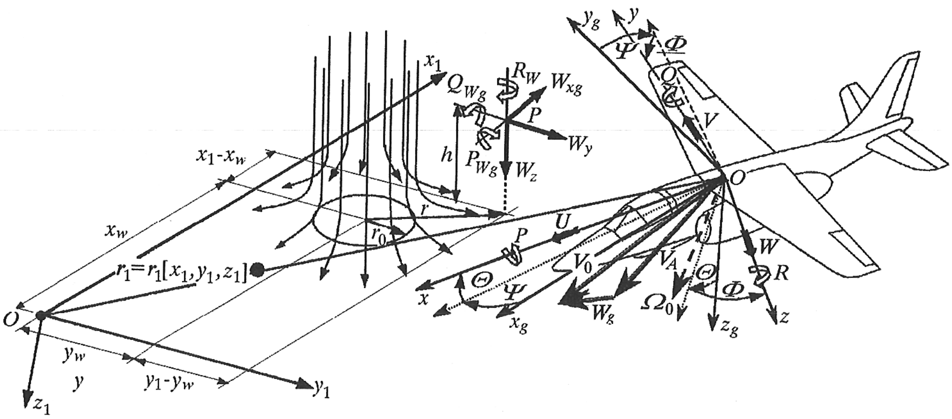

Fig. 1. Geometrical details of the microburst model

3. Physical and mathematical model of the aircraft

The following assumptions have been accepted:

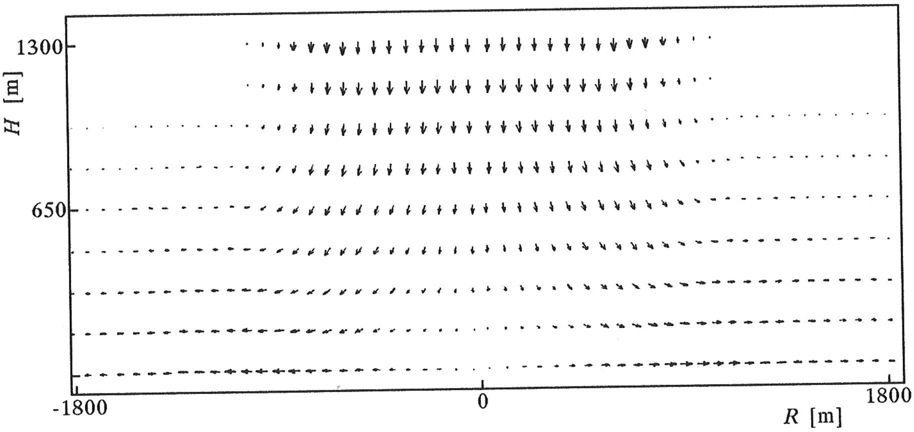

Fig. 2. Velocity vectors of the wind field in a radial cross-section (for parameters: $W_{Z_0} = 10\,\mathrm{m/s}$, $H_{ref} = 1000\,\mathrm{m}$, $R_0 = 600\,\mathrm{m}$)

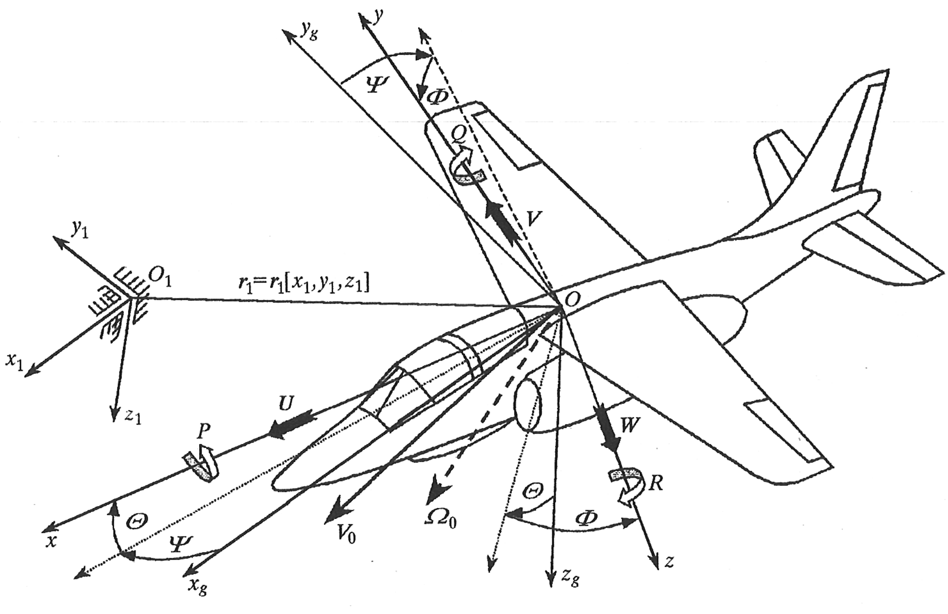

Fig. 3. Frames of reference: Earth-fixed, gravitational and body-fixed co-ordinate systems, respectively

- Aircraft is treated as a six degree-of-freedom rigid body. These degrees of freedom are represented by the linear displacements (x, y, z) and the angular movements written in terms of the Euler angles (Φ, Θ, Ψ) in the body-fixed co-ordinate system
- Aircraft flight is not controlled
- Quasi-stationary aerodynamics rules were employed for calculating of aerodynamic forces and moments
- Origin of the body-fixed co-ordinate system is located at 1 of the mean aerodynamic chord
- Earth rotation and its curvature are neglected.

The equations of motion (cf Maryniak, 1975; Frost, 1984) under windshear conditions are as follows:
— equation of the longitudinal motion

$$
\begin{aligned}
&m(\dot{U} + AW - RV) - S_x(Q^2 + R^2) + S_z(RP + \dot{Q}) = \\
&= -mg\sin\Theta + T_L\cos\varphi_{TyL} + T_P\cos\varphi_{TyP} + \\
&-\frac{1}{2}\rho S V_A^2(C_{xa}^W\cos\beta\cos\alpha + C_{ya}^W\sin\beta\cos\alpha - C_{za}^W\sin\alpha) + X_Q(Q - Q_W)
\end{aligned}
\tag{3.1}
$$

— equation of the lateral motion

$$
\begin{aligned}
&m(\dot{V} + RU - PW) + S_x(\dot{R} + PQ) - S_z(\dot{P} - RQ) = mg\cos\Theta\sin\Phi + \\
&+\frac{1}{2}\rho S V_A^2(-C_{xa}^W\sin\beta + C_{ya}^W\cos\beta) + Y_P(P - P_W) + Y_R(R - R_W) + Y_{\delta V}\delta_V
\end{aligned}
\tag{3.2}
$$

— equation of ascent

$$
\begin{aligned}
&m(\dot{W} + PV - QU) - S_x(\dot{Q} - RP) - S_z(P^2 + Q^2) = mg\cos\Theta\cos\Phi + \\
&-T_L\sin\varphi_{TyL} - T_P\sin\varphi_{TyP} + Z_{\alpha zH}\alpha_{zH} + Z_{\delta H}\delta_H + \\
&-\frac{1}{2}\rho S V_A^2(C_{xa}^W\cos\beta\sin\alpha + C_{ya}^W\sin\beta\sin\alpha - C_{za}^W\cos\alpha) + Z_Q(Q - Q_W)
\end{aligned}
\tag{3.3}
$$

— equation of rolling

$$
\begin{aligned}
&I_x\dot{P} - (I_y - I_z)QR - I_{xz}(\dot{R} + QP) + S_z(WP - RU - \dot{V}) = \\
&= -mgz_C \cos\Theta \sin\Phi - T_L y_{TL} \sin\varphi_{TyL} + \\
&+J_{TL}\omega_{TL} \sin\varphi_{TyL} - T_P y_{TP} \sin\varphi_{TyP} + J_{TP}\omega_{TP} \sin\varphi_{TyP} + \\
&-\frac{1}{2}\rho S V_A^2 \Big[c(C^W_{Mxa} \cos\beta \cos\alpha + C^W_{Mya} \sin\beta \sin\alpha - C^W_{Mza} \sin\alpha)\Big] + \\
&+L_P(P - P_W) + L_R(R - R_W) + L_{\delta V}\delta_V + L_{\delta L}\delta_L
\end{aligned}
\tag{3.4}
$$

— equation of pitching

$$
\begin{aligned}
&I_y\dot{Q} - (I_z - I_x)RP + S_z(\dot{U} - RV - WQ) - I_{xz}(R^2 - P^2) + \\
&-S_x(\dot{W} + PV - UQ) = -mg(z_C \sin\Theta + x_C \cos\Theta \cos\Phi) + \\
&+T_L(z_{TL} \cos\varphi_{TyL} + x_{TL} \sin\varphi_{TyL}) - J_{TL}\omega_{TL}(R \cos\varphi_{TyL} + P \sin\varphi_{TyL}) + \\
&+T_P(z_{TP} \cos\varphi_{TyP} + x_{TP} \sin\varphi_{TyP}) - J_{TP}\omega_{TP}(R \cos\varphi_{TyP} + P \sin\varphi_{TyP}) + \\
&+\frac{1}{2}\rho S V_A^2 \Big[c(-C^W_{Mxa} \sin\beta + C^W_{Mya} \cos\beta)\Big] + \\
&+M_Q(Q - Q_W) + M_{\dot{W}}(\dot{W} - \dot{W}_z) + M_{\alpha zH}\alpha_{zH} + M_{\delta H}\delta_H
\end{aligned}
\tag{3.5}
$$

— equation of the yawing motion

$$
\begin{aligned}
&I_z\dot{R} - (I_x - I_y)PQ - I_{zx}(\dot{P} - QR) + S_x(\dot{V} + PW - UR) = \\
&= mg(x_C \cos\Theta \sin\Phi + y_C \sin\Theta) + N_P(P - P_W) + N_R(R - R_W) + \\
&+N_{\delta V}\delta_V - T_L y_{TL} \cos\varphi_{TyL} + J_{TL}\omega_{TL} Q \cos\varphi_{TyL} + \\
&-T_P y_{TP} \cos\varphi_{TyP}) + J_{TP}\omega_{TP} Q \cos\varphi_{TyP} + \\
&-\frac{1}{2}\rho S V_A^2 \Big[c(C^W_{Mxa} \cos\beta \sin\alpha + C^W_{Mya} \sin\beta \sin\alpha + C^W_{Mza} \cos\alpha)\Big]
\end{aligned}
\tag{3.6}
$$

— kinematic formulae for the angular velocities

$$
\dot{\Phi} = P + (Q \sin\Phi + R \cos\Phi) \tan\Theta
$$

$$\dot{\Theta} = Q\cos\Phi - R\sin\Phi \tag{3.7}$$
$$\dot{\Psi} = (Q\sin\Phi + R\cos\Phi)\sec\Theta$$

— kinematic formulae for the linear velocities

$$\begin{aligned}
\dot{x}_1 &= U\cos\Theta\cos\Psi + V(\sin\Phi\sin\Theta\cos\Psi - \cos\Phi\sin\Psi) + \\
&+ W(\cos\Phi\sin\Theta\cos\Psi + \sin\Phi\sin\Psi) \\
\dot{y}_1 &= U\cos\Theta\sin\Psi + V(\sin\Phi\sin\Theta\sin\Psi + \cos\Phi\cos\Psi) + \\
&+ W(\cos\Phi\sin\Theta\sin\Psi - \sin\Phi\cos\Psi) \\
\dot{z}_1 &= -U\sin\Theta + V\sin\Phi\cos\Theta + W\cos\Phi\cos\Theta
\end{aligned} \tag{3.8}$$

— flight altitude

$$h = -z_1 \tag{3.9}$$

— atmospheric density for $h \leqslant 11000\,\mathrm{m}$

$$\rho = \rho_0\Big(1 + \frac{z_1}{44300}\Big)^{4.256} \tag{3.10}$$

— velocity of the aircraft

$$V_0 = \sqrt{U^2 + V^2 + W^2} \tag{3.11}$$

— angle of attack with the air motion considered

$$\alpha = \arcsin\frac{W - W_z}{V_A} \tag{3.12}$$

— angle of sideslip with the air motion considered

$$\beta = \arcsin\frac{V - W_y}{V_A} \tag{3.13}$$

— velocity relative to the air

$$V_A = \sqrt{(U - W_x)^2 + (V - W_y)^2 + (W - W_z)^2} \tag{3.14}$$

— equation of motor rotation

$$n_T = K_1^T(\mathrm{Ma}, \tau, \rho_H)\frac{n_{\max} - n_0}{\delta_{T\max}} \tag{3.15}$$

— equation of thrust

$$T = K_2^T(\mathrm{Ma})\frac{T_{\max} - T_0}{n_{\max} - n_0} \tag{3.16}$$

— angular velocity of the engine-turbocompressor assembly

$$\omega_T = \frac{2\pi}{60} n_T \tag{3.17}$$

The dynamical equations of the aircraft motion were derived in the body-fixed co-ordinate system. After certain transformations and reductions, the equations of motion can be rewritten in a matrix form

$$\dot{\boldsymbol{V}} = \widetilde{\mathbf{M}}^{-1}(\boldsymbol{Q} - \boldsymbol{K}\mathbf{M}\boldsymbol{V}) \tag{3.18}$$

where

$\widetilde{\mathbf{M}}$	–	modified matrix of inertia, $\widetilde{\mathbf{M}} = \mathbf{M} + \mathbf{M}_{\dot{\boldsymbol{W}}}$
$\boldsymbol{V}$	–	vector of velocities, $\boldsymbol{V} = [U, V, W, P, Q, R]^\top$
$\dot{\boldsymbol{V}}$	–	vector of accelerations
$\boldsymbol{Q}$	–	vector of external forces, $\boldsymbol{Q} = [X, Y, Z, L, M, N]^\top$.

When taking the wind field into consideration, the dimensionless coefficients of aerodynamic forces and moments depend on the angles of attack and sideslip, respectively, as well as on the Mach and Reynolds numbers

$$C_x^W,\ C_y^W,\ C_z^W,\ C_L^W,\ C_M^W,\ C_N^W, = f(\alpha, \beta, \mathrm{Ma}, \mathrm{Re})$$

4. Numerical simulation

Numerical simulation was performed to analyse the microburst effect on the aircraft dynamics. To show what factors affect the aircraft behaviour, the computations were made assuming the following cases:

- To consider the initial velocity effect for $W_{Z_0} = 10\,\mathrm{m/s}$, $H_0 = 400\,\mathrm{m}$, $Y_W = 100\,\mathrm{m}$; three initial velocities of the aircraft were analysed: $V_0 = 400\,\mathrm{km/h}$, $V_0 = 560\,\mathrm{km/h}$, $V_0 = 720\,\mathrm{km/h}$.
- To consider the wind field effect for $V_0 = 560\,\mathrm{km/h}$, $H_0 = 400\,\mathrm{m}$, $Y_W = 100\,\mathrm{m}$ the following vertical components of wind velocity of reference were analysed: $W_{Z_0} = 10\,\mathrm{m/s}$, $W_{Z_0} = 15\,\mathrm{m/s}$, $W_{Z_0} = 20\,\mathrm{m/s}$.

Having courses of the wind velocity components vs. time, the following three phases can be distinguished in the aircraft motion:

- At the first stage the aircraft encounters the headwind and crosswind, therefore the aircraft starts climbing. As a result, its velocity is reduced. This phase lasts until the vertical component of wind velocity appears.

- Second phase lasts between 45th and 53rd second (for $V_0 = 560\,\mathrm{km/h}$). In that time the pitch rate is greater than in the first phase of flight. The pitch attitude and the altitude change more quickly.
- In the third phase, after crossing the centre of the microburst W_{xg}, the wind velocity component changes its sign (tailwind). This component causes diminishing of the altitude. After this phase the aircraft motion assumes oscillatory character.

5. Conclusions

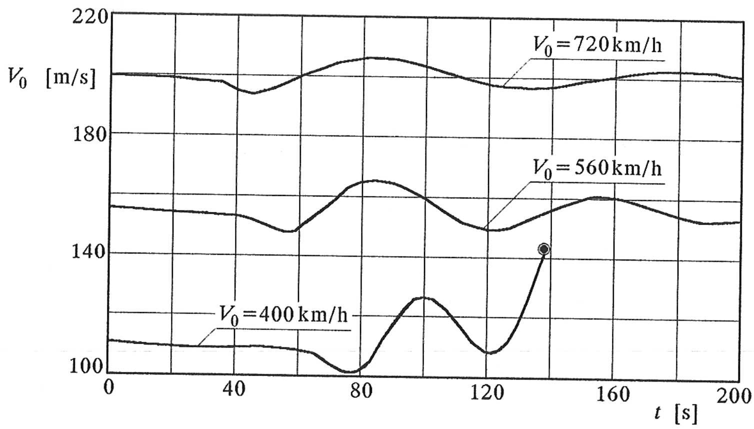

Fig. 4. Aircraft velocity courses vs time for different initial aircraft velocities; $W_{Z_0} = 10\,\mathrm{m/s}$, $H_0 = 400\,\mathrm{m}$, $X_W = 8000\,\mathrm{m}$, $Y_W = 100\,\mathrm{m}$

The numerical simulation of the flight through the microburst, which have been performed shows that this phenomenon can be dangerous not only for large planes (Dietenberger, 1985; Jimoh, 1992), but also for smaller ones of the I-22 "Iryda" class. The investigations reveal that the vertical component of wind velocity is the critical one which affects the safety of a flight (Fig.6 ÷ Fig.8), and the aircraft velocity before encountering of the microburst (Fig.4 ÷ Fig.7). The angle of attack increases in area of occurrence of a vertical wind (for $W_{Z_0} = 20\,\mathrm{m/s}$ and $V_0 = 560\,\mathrm{km/h}$ this angle increases up to 11°, but for $W_{Z_0} = 10\,\mathrm{m/s}$ and $V_0 = 400\,\mathrm{km/h}$ the aircraft crashes). Large oscillations of the pitch rate appear (Fig.5). The simulation shows that the vertical component of wind velocity does not have to be high to maintain

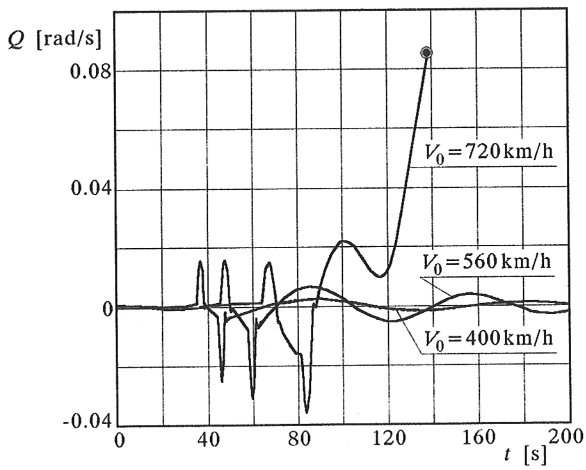

Fig. 5. Pitch rate courses vs time for different V_0; $W_{Z_0} = 10\,\mathrm{m/s}$, $H_0 = 400\,\mathrm{m}$, $X_W = 8000\,\mathrm{m}$, $Y_W = 100\,\mathrm{m}$

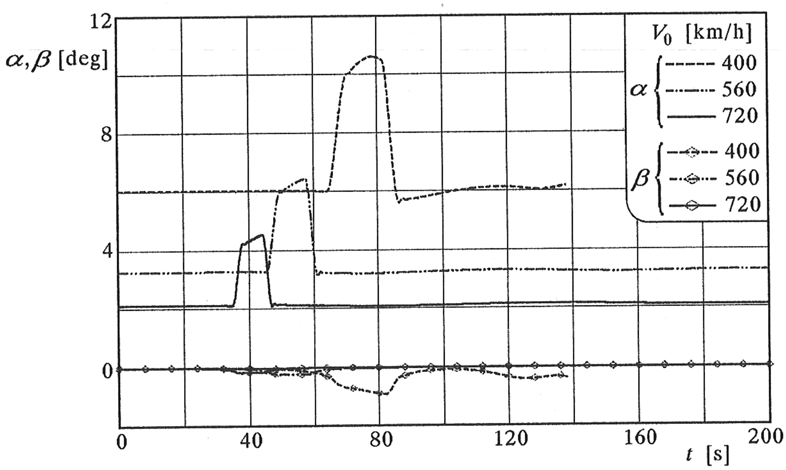

Fig. 6. Angle of attack and sideslip angle courses, respectively, for different V_0; $W_{Z_0} = 10\,\mathrm{m/s}$, $H_0 = 400\,\mathrm{m}$, $X_W = 8000\,\mathrm{m}$, $Y_W = 100\,\mathrm{m}$

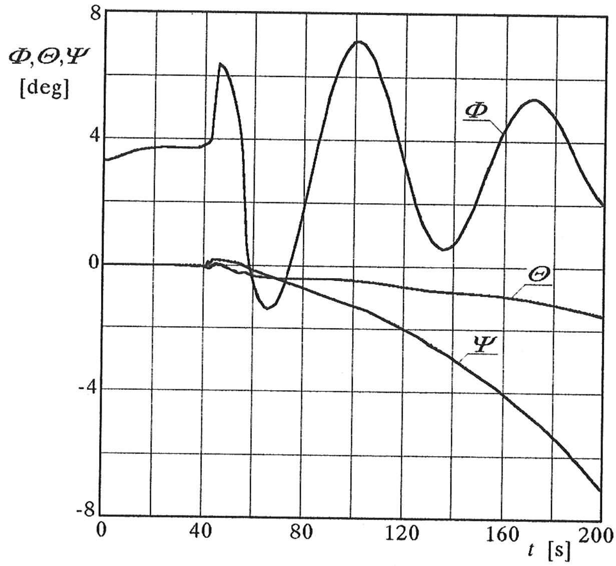

Fig. 7. Attitudes of pitch, yaw, and roll for different V_0; $W_{Z_0} = 10\,\mathrm{m/s}$, $H_0 = 400\,\mathrm{m}$, $X_W = 8000\,\mathrm{m}$, $Y_W = 100\,\mathrm{m}$

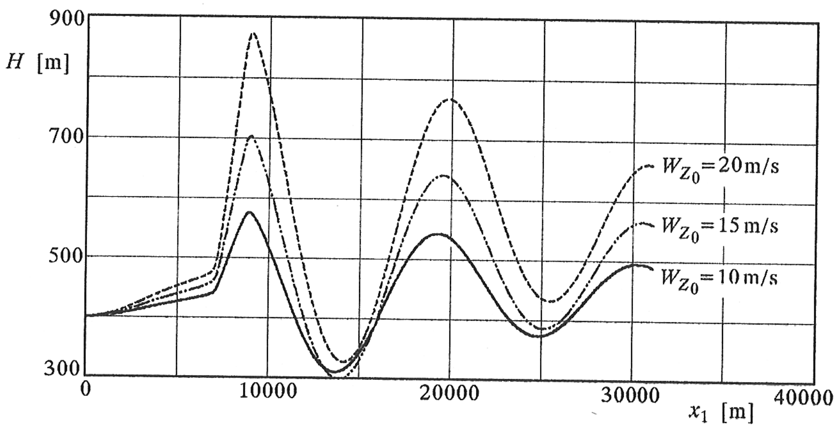

Fig. 8. Altitudes along the x_1-axis for different W_{Z_0}; $V_0 = 560\,\mathrm{km/h}$, $H_0 = 400\,\mathrm{m}$, $X_W = 8000\,\mathrm{m}$, $Y_W = 100\,\mathrm{m}$

the safety of flight. The constructed physical and mathematical model of the aircraft including the microburst effect on the aircraft dynamics reveals the following advantages:

- It is simple and general.
- Modular structure of the simulation program allows for making the model more detailed, e.g., including the autopilot response, etc.
- Certain dynamic characteristics, the in flight examination of which is very difficult for safety and economical reasons can be analysed.
- Model can be applied to any subsonic and undeformable aircraft.
- Size and intensity of the wind-flow can be easy regulated by changing three parameters: height of reference H_{ref}, radius defining the contour of maximum vertical velocities R_0 and vertical component of the wind velocity reference W_{Z_0}.

The work was supported by the State Committee for Scientific Research under grant No 9 T12C 018 13.

References

1. ASSELIN M., 1997, *An Introduction to Aircraft Performance*, John Wiley and Sons Inc., NY
2. DIETENBERGER M., 1985, Reconstruction of Pan Am New Orleans Accident, *Journal of Aircraft*, **22**, 8, 719-728
3. FISZDON W., 1961, *Mechanika lotu*, PWN, Łódź-Warszawa
4. FROST W., 1984, Wind Shear Term in the Equations of Aircraft Motion, *Journal of Aircraft*, **21**, 11, 866-872
5. FROST W., HO-PEN CHANG, 1985, Aircraft Performance in a JAWS Microburst, *Journal of Aircraft*, **22**, 7, 561-567
6. GOSZCZYŃSKI J.A., PYRZ J., 1997, Wyznaczenie pochodnych aerodynamicznych samolotu I-22 z wykorzystaniem badań tunelowych, ESDU i innych metod obliczeniowych, *Proceedings Institute of Aviation*, Warsaw, 248/SZ-OA/97
7. IVAN M., 1986, A Ring-Vortex Downburst Model for Flight Simulations, *Journal of Aircraft*, **23**, 3, 232-236

8. JIMOH O.P., 1992, Badania symulacyjne reakcji samolotu pasażerskiego w locie przestrzennym po wejściu w zmienny podmuch, Ph.D. thesis, Warsaw University of Technology, Warsaw

9. MARYNIAK J., 1975, Dynamiczna teoria obiektów ruchomych, *Prace Naukowe PW, Mechanika*, **3**, WPW, Warsaw

10. MARYNIAK J., 1987, Modelowanie fizyczne i matematyczne w dynamice obiektów ruchomych, *XXVI Sympozjum Modelowanie w Mechanice, Zeszyty Naukowe Politechniki Śląskiej*, **XX**, Gliwice

Symulacja numeryczna lotu samolotu po przejściu przez podmuch typu "microburst"

Streszczenie

W pracy przedstawiono fizyczne i matematyczne modelowanie wpływu podmuchu *microburst* na dynamikę samolotu. Dynamiczne równania ruchu obiektu wyprowadzono w układzie sztywno związanym z samolotem, stosując zapis Boltzmanna-Hamela dla układów mechanicznych o więzach holonomicznych. Samolot potraktowano jako bryłę sztywną o sześciu stopniach swobody. Symulację wykonano dla fazy lotu poziomego z trzymanymi sterami. Obliczenia zmian sił aerodynamicznych i momentów sił aerodynamicznych wykonano w oparciu o aerodynamikę quasistacjonarną. Pole prędkości podmuchu *microburst* opisano w pełni trójwymiarowym modelem matematycznym Braya, opracowanym na bazie danych metorologicznych z projektu badawczego Joint Airport Weather Studies z 1982 roku w USA. Wpływ parametrów lokalnych pola wiatru w równaniach ruchu obiektu latającego uwzględniono przez trzy chwilowe liniowe składowe wektora prędkości podmuchu i trzy chwilowe kątowe składowe tegoż wektora. W pracy przeanalizowano zachowanie się samolotu po przelocie mimośrodowym przez obszar podmuchu dla różnych parametrów charakteryzujących uskok wiatru. Wykazano, że składowa pionowa prędkości wiatru nie musi być wielka, aby zagrozić bezpieczeństwu lotu. Jako samolot testowy wybrano PZL I-22 "Iryda".

Manuscript received March 28, 2000; accepted for print June 14, 2000